forum acusticum 2026
8-12 September · Graz, Austria

OPTIMIZING MICROPERFORATED METAMATERIAL PANELS IN THE WHEEL-ARCH FOR TIRE/ROAD NOISE REDUCTION: NUMERICAL APPROACH

R. Mafféïs[1], J. Picaut[1], R. Picó[2]

[1] *Univ. Gustave Eiffel, Cerema, UMRAE, F-44344 Bouguenais, France*
[2] *Instituto de Investigacion para la Gestion Integrada de Zonas Costeras, Universitat Politecnica de Valencia, C. Paranimf, 1, Gandia, 46730, Spain*

This paper is a revised version of the authors' submitted manuscript that was peer-reviewed by at least two anonymous reviewers.

Abstract

This study proposes the use of an acoustic metamaterial in the wheel arch to reduce the noise generated by tire-road contact. The method employed is based primarily on the use of a simplified numerical model of a wheel arch that combines finite elements with boundary elements to evaluate the impact of an acoustic absorption treatment in this area. Based on this assessment, an acoustic metamaterial consisting of parallel micro-perforated panels is selected and optimized to achieve the target performance in terms of absorption, dimensions, and frequency range. Finally, the expected absorption coefficient is verified by several ways, using an analytical model, a numerical model, and a Kundt tube based measurements of the 3D-printed model. The obtained results pave the way for full-scale evaluation of such metamaterial device in a wheel arch.

Keywords: *tire/road noise, acoustic metamaterial, microperforated panel, absorption coefficient*

1. Introduction

Road traffic noise is currently the noise source that causes the most harm in terms of its impact on health in Europe [1]. Generally speaking, road traffic noise consists of two sources: propulsion noise and tire/road noise. Above a speed of 50 km/h, tire/road noise —which results from the interaction between the road surface and the tire— becomes dominant over propulsion noise [2].

Since the latter results from numerous airborne, vibrational, and amplification mechanisms, the road noise spectrum peaks around 1 kHz, which is particularly annoying to the human ear [3]. The gradual electrification of the vehicle fleet, leading to the decrease of propulsion noise [4], requires consideration of more effective means to reduce tire/road noise.

Furthermore, the field of acoustic metamaterials, which has been developing for several years, offers new ways to reduce noise through structures with acoustic properties that cannot be achieved using conventional materials such as porous materials [5]. One of the key characteristics is their ability to achieve high sound absorption while maintaining subwavelength dimensions [5, 6]. Especially metamaterials using microperforated panels (MPP) have demonstrated broadband absorption capabilities, while featuring analytical models that are easy to implement and dimensions that are relatively small compared to the wavelength [7–9].

In this context, the application of acoustic metamaterials in the automotive sector has primarily focused on reducing interior noise rather than noise emitted to the outside [10–15]. Nevertheless, research has demonstrated the possibility of reducing radiated noise through the use of porous materials, micro-perforated panels (MPP), or quarter-wave resonators based metamaterial on certain parts of the vehicle, such as the underbody and wheel arch [16–20]. These reductions are estimated at 1 to 2 dB in pass-by measurements [21].

In this paper, we present a preliminary numerical and experimental study aimed at proposing a simple structure based on acoustic metamaterials to reduce tire/noise at the source, focusing on acoustic treatment within the wheel arch (Figure 1). Numerical results obtained using a simplified finite element model of a wheel arch are first compared with results from the literature in terms of the gain between a fully absorptive acoustic treatment and a perfectly reflecting surface inside the wheel well (Section 2). An acoustic metamaterial composed of parallel micro-perforated panels backed by cavities is then optimized to approx-

Corresponding author: *robin.maffeis@univ-eiffel.fr.*

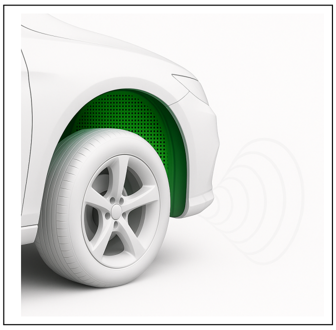

Figure 1: Representation of the concept of MPP in the wheel arch - AI generated.

imate the theoretically complete absorption over a given frequency range (Section 3). These optimization results are subsequently compared with finite element simulations and with measurements in terms of absorption coefficients. Lastly, Section 4 concludes on this study.

2. Numerical evaluation of an acoustic treatment in a wheel arch

2.1. Wheel arch numerical model

In order to study the behavior of the wheel arch and reproduce the real geometry based on Figure 1, a simple numerical model of a single wheel arch (Figure 2a) was created.

The objective is to calculate the field radiated at a receiving point, according to ISO362-1:2022 standard [21], *i.e.* 7.5 m perpendicularly to the vehicle and 1.2 m high as presented on Figure 2b.

The volumes shown in Figure 2a represent the air domain within the model. The blue region corresponds to the area where a specific impedance boundary condition is applied. All other surfaces, including the ground, are modeled using a Neumann boundary condition. In order to evaluate the effect of a fully absorbent treatment in the blue area, a perfectly matched boundary (PMB) condition is used [22]. Finally, tire/road noise is modeled by considering two monopoles in phase, with a pressure amplitude of 1 Pa each, a height of 1 mm and separated by 20 cm [23].

The propagation model combines finite elements (FEM) with boundary elements (BEM): the interior of the domain is solved using finite elements, while the outer faces are coupled with boundary elements. This coupling allows radiated noise to be propagated over a distance, thereby enabling the assessment of noise reduction at the selected receiving point, as shown in Figure 2b.

2.2. Effect of an acoustic treatment

Based on this simplified model, a comparison is made in Figure 3 between what can be considered as two extreme cases: a Neumann-type condition (*i.e.* perfectly reflecting boundaries, the reference case) and a PMB condition (*i.e.* perfectly absorbing boundaries) applied to the treatment area. The idea is to evaluate

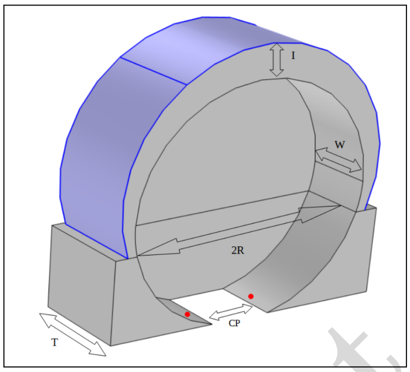

(a) Numerical model of the wheel arch: blue region represents surfaces where a specific impedance is defined; red dots indicate the position of the two monopoles thats simulates the tire/road noise emission.

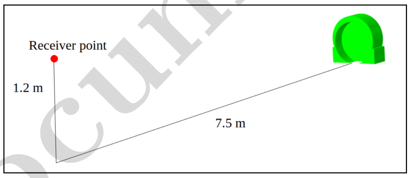

(b) Geometrical configuration for the estimation of tire/road noise at a recevier point from the receiver point.

Figure 2: Numerical model of the wheel arch and geometrical configuration for the evalaution of the tire/road noise level: tire radius is R = 32.5 cm, tire width is W = 19 cm, the distance between the wheel arch and tire is I = 10 cm, the contact patch length is CP = 16 cm and wheel arch width is T = 30 cm.

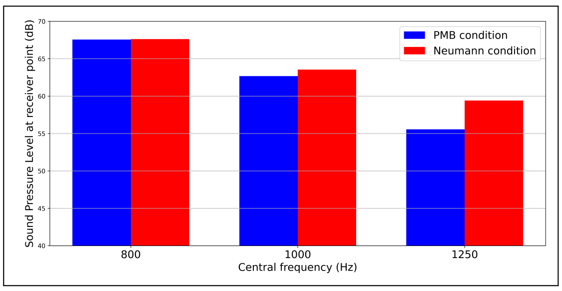

Figure 3: Sound pressure level at the receiver point with different impedance condition in the wheel arch: PMB (blue) and Neumann conditions.

the maximum achievable gain for this type of treatment. The calculation is performed across the three third-octave bands from 800 to 1250 Hz. The gain for the third-octave 800 Hz is negligible, while gains of 1 dB and 3 dB, respectively, are calculated for the 1000 and 1250 Hz third-octave bands.

This result of 1 dB around 1000 Hz is consistent with previously reported results in the literature involving micro-perforated panels, quarter-wave resonators and porous materials [18, 19].

The results obtained in the 1250 Hz band, which are higher than those in the 1000 Hz band, can be explained, on the one hand, by absorption in the wheel well and, on the other hand, by destructive interference resulting from the problem's geometry. This effect is further accentuated by the fact that for the reference extreme case all surfaces are considered reflective, which tends to increase the amplitude of the interference.

Although these results appear relatively modest in terms of noise reduction, it is important to note that European regulations regarding pass-by noise emissions are becoming increasingly stringent [24], requiring the automotive industry to seek effective solutions for reducing noise. Furthermore, achieving additional noise reduction by addressing other parts of the vehicle can lead to a significant overall reduction.

Based on these numerical estimates of the potential noise reduction for a fully absorbing treatment, the goal is to develop an acoustic metamaterial capable of achieving acoustic performance close to these estimates within the target frequency band of the tire/road noise spectrum, while maintaining a relatively small size due to the constrained environment. In the next section, an acoustic metamaterial is proposed as a possible solution for an acoustic treatment in the wheel arch.

3. Metamaterial stucture

3.1. Analytical model

The proposed metamaterial consists of MPP arranged in parallel, backed by cavities of various depths (Figure 4b).

-

A MPP can be modeled by a local impedance that takes into account wave propagation in small conduits, including thermoviscous effects. The Maa model [7, 25] allows this impedance to be modeled using the following simplified formula:

$$Z_{\mathrm{MPP}} = -\frac{j\omega\rho_0 \mathrm{t}}{\phi}\,\sigma_i + \frac{32\eta \mathrm{t}}{\phi \mathrm{d}^2}\,\sigma_\tau, \tag{1}$$

where t is the thickness of the plate, ϕ is the porosity defined as $\phi = \mathrm{N_h}\frac{\pi \mathrm{d}^2}{\mathrm{D}^2}$ with D being the size of the unit cell and $\mathrm{N_h}$ the number of hole, d is the diameter of the perforations, ρ_0 is the air density, ω is the pulsation and η the dynamic viscosity of air. The coefficients

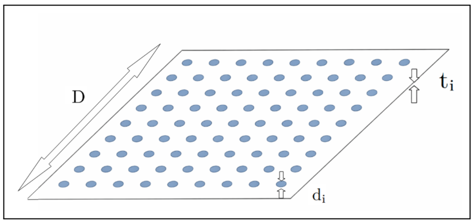

(a) Micro-perforated panels (MPP) geometry description.

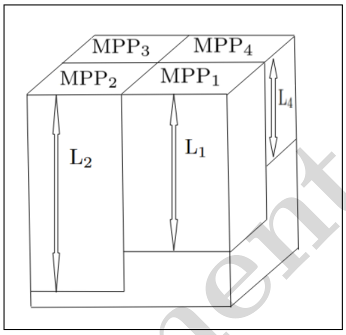

(b) Arrangments of multiple MPP on cavities with specific depths.

Figure 4: Metamaterial structure based on a MPP arrangements on cavities.

σ_i and σ_τ are expressed by

$$\sigma_i = 1 + \left[1 + \frac{\sigma^2}{2}\right]^{-\frac{1}{2}} + 0.85\frac{\mathrm{d}}{\mathrm{t}}, \tag{2}$$

and

$$\sigma_\tau = \sqrt{1 + \frac{\sigma^2}{32} + \frac{4\sqrt{2}}{32}\sigma\frac{\mathrm{d}}{\mathrm{t}}}. \tag{3}$$

This formula is valid in the case where $1 \leq \sigma \leq 10$ with $\sigma = \mathrm{d}\sqrt{\omega\rho_0/4\eta}$. These structures are coupled to cavities so that the total impedance of the structure is as follows:

$$Z = Z_{\mathrm{MPP}} + Z_c, \tag{4}$$

with the impedance of the cavity defined by

$$Z_c = -j\rho_0 c_0 \cot(\omega \mathrm{L}/c_0), \tag{5}$$

where L and c_0 are respectively the lenght of the cavity and the speed of sound in the air.

The advantage of this type of structure, unlike quarter-wave or Helmholtz resonators, is that it allows for a broader bandwidth while maintaining relatively high absorption [7]. In the case of structures coupled in parallel, as presented in Figure 4b, the total impedance of the N units with different surface proportions can be calculated using the admittance sum method [26]:

$$Z_{\mathrm{tot}} = (\sum_{n=1}^{\mathrm{N}} \frac{1}{\mathrm{N}}\frac{1}{Z_n})^{-1}, \tag{6}$$

where N and Z_n are respectively the number of cell

Parameter	w	c_1	c_2	pop. size	n
PSO	0.7298	1.49618	1.49618	150	2000

Table 1: PSO algorithm parameters used for optimization

Parameter	ϕ	d (mm)	t (mm)	L (mm)
MPP_1	0.0364	0.93 (0.9)	2	20 (20)
MPP_2	0.0176	0.92 (0.9)	2	19.9 (20)
MPP_3	0.0251	0.90 (0.9)	2	20 (20)
MPP_4	0.0148	1.00 (1.0)	2	19.8 (20)

Table 2: Geometric parameters of the metamaterial after optimization - The values in parentheses are the values used for 3D printing.

and the impedance of the n^{th} microperforated panel. Finally, the sound absorption coefficient at normal incidence is calculated using the following expression:

$$\alpha = 1 - |\frac{Z_{\text{tot}} - \rho_0 c_0}{Z_{\text{tot}} + \rho_0 c_0}| \qquad (7)$$

In the case of the study, the number of cells N is fixed to 4.

3.2. Metamaterial optimization

The optimization problem consists in maximizing the metamaterial absorption over a target frequency range $[f_1, f_2]$ and an incidence angle range $[\theta_1, \theta_2]$. To do this, the objective is to minimize the function Φ defined as follows:

$$\min_{\mathbf{x}} \Phi = -\frac{1}{(\theta_2 - \theta_1)(f_2 - f_1)} \int_{\theta_1}^{\theta_2} \int_{f_1}^{f_2} \alpha(\theta, f, \text{x}), \qquad (8)$$

with x being the parameter vector defined as

$$\mathbf{x} = (\phi_{\text{i}},\ \text{d}_{\text{i}},\ \text{t}_{\text{i}},\ \text{L}_{\text{i}}), \qquad (9)$$

with i corresponding to the i^{th} micro-perforated panel, as described on Figure 4b. To reduce the number of variables to be optimized, we assume that the panels have the same thickness t.
The algorithm used is based on the Particle Swarm Optimization (PSO) procedure proposed by [27] and inspired by social behavior. Based on [28–30], the chosen algorithm parameters are listed in Table 1 in order to ensure numerical convergence. For this work, the target frequency range is included between 800 and 1300 Hz while the angle range is from 0° to 88°. Finally, Table 2 gives the optimized parameters of the metamaterial.

3.3. Experimental evaluation

A 3D-printed sample of the model is manufactured and measured in a Kundt tube in order to determine the absorption coefficient in accordance with standard ISO 10534 [31]. Figure 5a shows the experimental setup, which consists mainly of a power amplifier, a signal generator, two 1/4-inch microphones, and a square-section impedance tube. The inner dimension of the impedance tube is 50 mm. The tested sample made of polylactic acid (PLA), has the following dimensions: 4.9 cm on each side and 2.2 cm (*i.e.* L + d) in height,

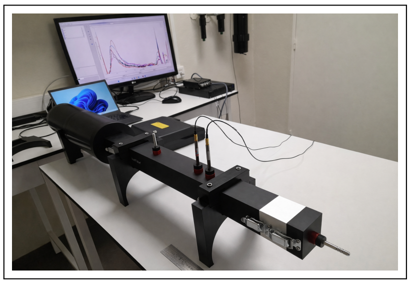

(a) Kundt Tube.

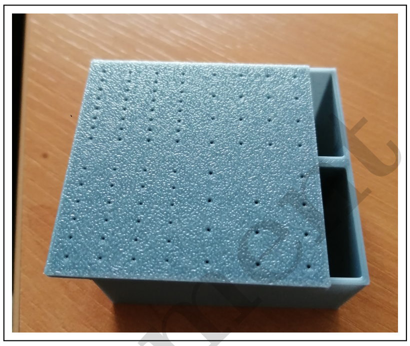

(b) MPP based metamaterial 3D printed - dimensions are presented on Table 2.

Figure 5: Experimental set-up measurement of microperforated panel absorption coefficient.

as shown in Figure 5b. Due to printing errors, some of the holes are blind or have diameters smaller than prescribed, which alters the acoustic impedance of the MPP and reduces their absorption performance. To avoid this problem, the panels are mechanically drilled to match the optimized diameter, rounded to 0.1 mm [32].

3.4. Finite element model implementation

A numerical model was also developed using COMSOL Multiphysics v6.3 finite element software to calculate the absorption coefficient of the metamaterial.
A square tube with four independent cavities at its end, along with MPPs, is modeled. The MPPs are simulated using an equivalent impedance condition for a perforated panel, which requires the panel thickness, the hole diameter, and surface porosity. The bottom of the cavities is assigned a Neumann boundary condition, while a plane wave propagated through the tube. A maximum mesh size criterion of $\lambda/10$ is applied to reduce numerical errors.

3.5. Results

The absorption coefficients obtained from measurements, the analytical solution and the numerical model, with the optimized parameters are compared in Figure 6.
Overall, there is good agreement, with absorptions around 0.9 in the optimized frequency range. However, it appears that the absorption coefficient obtained from the measurement is missing one peak at f = 1100 Hz. This effect can be explained by uncertainties

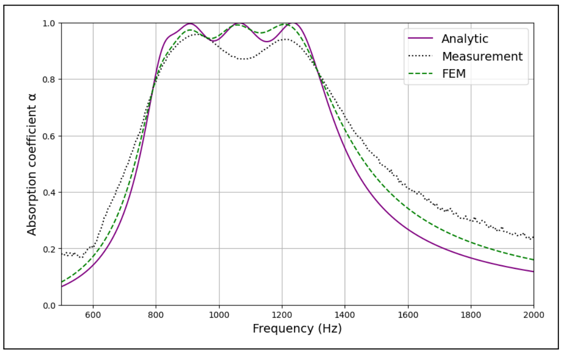

Figure 6: Comparison of the absorption coefficient of the micro-perforated panel based metamaterial: analytical, FEM and experimental results.

in the printing and drilling processes, which can affect the actual diameter and, consequently, the porosity of the cell. As a result, a peak corresponding to the resonance of one of the cells may overlap with another peak due to manufacturing errors.

4. Conclusion

Using a numerical model of a simplified wheel arch that combines finite elements and boundary elements, simulations were performed to evaluate the noise-reduction potential of installing sound-absorbing material inside the wheel arch.

Based on these simulations, which yielded results of the same order of magnitude as those reported in the literature, a metamaterial was designed to approximate perfect absorption within the target frequency band. Due to practical considerations and the constrained environment, the choice was made to use four micro-perforated panels in parallel backed by cavities. The absorption coefficient of the metamaterial was optimized over a frequency band ranging from 800 to 1300 Hz using a particle swarm optimization algorithm.

The resulting geometry was then 3D printed and the absorption coefficient was measured and compared to analytical and numerical results, with success, confirming the acoustic characteristics of the expected treatment of the wheel arch.

The advantage of this method is that it offers a compact metamaterial that is easy to fabricate and adjust, while delivering gains on the same order of magnitude as those reported in the literature.

Based on these results, the objective is now to evaluate by full-scale measurements the real effect of such metamaterial based acoustic treatment, in terms of noise reduction at a receiver close to the vehicle, when considering a full treatment of the wheel arch with such metamaterial device.

5. Acknowledgments

The authors would like to thank UMRAE laboratory members (Philippe Glé, Clément Piegay, Laurent Brendel, Nicolas Fortin, Vincent Gary), as well as Yannick Falaise (Univ. Gustave Eiffel) for the absorption coefficient measurements and 3D printing supports. This research was partially developed under grant PID2022-138321NBC22 funded by MICIU/AEI/10.13039/501100011033 and ERDF/EU.

References

[1] European Environment Agency, "Environmental noise in europe — 2025," European Environment Agency, Tech. Rep., 2025.

[2] T. Li, "Literature review of tire-pavement interaction noise and reduction approaches," *Journal of Vibroengineering*, vol. 20, no. 6, pp. 2424–2452, 2018.

[3] U. Sandberg, "The multi-coincidence peak around 1000 hz in tyre/road noise spectra," *Euronoise Naples*, vol. 89, no. 1-8, p. 2019, 2003.

[4] S. Baclet, J. Nygren, and R. Rumpler, "Impact of car electrification on urban noise pollution: A microscopic traffic simulation study," in *INTER-NOISE and NOISE-CON congress and conference proceedings*, Institute of Noise Control Engineering, vol. 270, 2024, pp. 7846–7855.

[5] G. Comandini, M. Ouisse, V. Ting, and F. Scarpa, "Architected acoustic metamaterials: An integrated design perspective," *Applied Physics Reviews*, vol. 12, no. 1, 2025.

[6] Y. Tang, F. Xin, L. Huang, and T. Lu, "Deep subwavelength acoustic metamaterial for low-frequency sound absorption," *Europhysics Letters*, vol. 118, no. 4, p. 44 002, 2017.

[7] D.-Y. Maa, "Potential of microperforated panel absorber," *The Journal of the Acoustical Society of America*, vol. 104, no. 5, pp. 2861–2866, 1998.

[8] P. Soon-Hong, "A design method of micro-perforated panel absorber at high sound pressure environment in launcher fairings," *Journal of Sound and Vibration*, vol. 332, no. 3, pp. 521–535, 2013.

[9] C. R. Liu, J. H. Wu, Z. Yang, and F. Ma, "Ultra-broadband acoustic absorption of a thin microperforated panel metamaterial with multi-order resonance," *Composite Structures*, vol. 246, p. 112 366, 2020.

[10] K.-J. Chang, J. Jung, H.-G. Kim, D. R. Choi, and S. Wang, "An application of acoustic metamaterial for reducing noise transfer through car body panels," in *10th International Styrian Noise, Vibration & Harshness Congress: The European Automotive Noise Conference*, SAE Technical Paper, 2018.

[11] K.-J. Chang, N. G. Rocha de Melo Filho, L. Van Belle, C. Claeys, and W. Desmet, "A study on the application of locally resonant acoustic metamaterial for reducing a vehicle's engine noise," in *INTER-NOISE and NOISE-CON congress and conference proceedings*, Institute of Noise Control Engineering, vol. 259, 2019, pp. 102–113.

[12] J. Daniel, "Automotive wheel and tyre design for suppression of acoustic cavity noise through the incorporation of passive resonators," *Journal of Sound and Vibration*, vol. 467, p. 115 037, 2020.

[13] L. Sangiuliano, R. Boukadia, E. Deckers, W. Desmet, and C. Claeys, "Reduction of structure-borne tyre/road noise through rubber resonant metamaterials in tyres," *SAE International Journal of Advances and Current Practices in Mobility*, vol. 5, no. 2022-01-0954, pp. 909–920, 2022.

[14] H. Kojima and S. Suzuki, "Study on the install location of acoustic metamaterials absorbing tire noise," in *Proceedings of the Aachen Acoustics Colloquium 2024*, 2024.

[15] P. R. Gunreddy and M. Leamy, "Split ring resonator-based metamaterial with total bandgap for reducing nvh in electric vehicles," SAE Technical Paper, Tech. Rep., 2024.

[16] B. R. Wyerman and G. C. Jay, "Tire noise reduction with fiber exterior wheel arch liners," in *SAE 2007 Noise and Vibration Conference and Exhibition*, SAE Technical Paper, 2007.

[17] P. Gilotte and B. Surowiec, "Tyre road noise acoustic reduction due to rear wheel arch absorption," in *INTER-NOISE and NOISE-CON Congress and Conference Proceedings*, Institute of Noise Control Engineering, vol. 247, 2013, pp. 3424–3433.

[18] T. Lafont, J. Horak, R. D'Amico, R. Stelzer, and C. Bertolini, "Passive treatment solutions for the reduction of vehicle exterior tire noise. 10th international styrian noise," in *Vibration & Harshness Congress, June*, pp. 20–22.

[19] F. Kronowetter et al., "Novel compound material and metamaterial wheelhouse liners for tire noise reduction," *Mechanical Systems and Signal Processing*, vol. 200, p. 110 548, 2023.

[20] Y. Gültekin, T. Jean, M. A. Akar, and U. Kumlu, "Investigation of micro-perforated plate structure and cavity used as helmholtz resonator in wheel arch liner," *European Mechanical Science*, vol. 9, no. 1, pp. 38–45, 2025.

[21] International Organization for Standardization, *Acoustics — engineering method for measurement of noise emitted by accelerating road vehicles*, Geneva: ISO, 2022. [Online]. Available: `https://www.iso.org/standard/80872.html`.

[22] J.-P. Berenger, "A perfectly matched layer for the absorption of electromagnetic waves," *Journal of Computational Physics*, vol. 114, no. 2, pp. 185–200, 1994.

[23] T. Lafont, R. Stelzer, R. D'Amico, C. Bertolini, and W. Kropp, "Modeling tyre noise in fe simulations for pass-by noise predictions," in *Proceedings of NOVEM 2018 (Noise and Vibration Emerging Methods)*, Ibiza, Spain, 2018.

[24] United Nations Economic Commission for Europe (UNECE), *Regulation no. 51 of the economic commission for europe of the united nations (unece): Uniform provisions concerning the approval of motor vehicles having at least four wheels with regard to their sound emissions*, Official Journal of the European Union, 2018.

[25] D.-Y. Maa, "Microperforated-panel wideband absorbers," *Noise Control Engineering Journal*, vol. 29, no. 3, pp. 77–84, 1987.

[26] K. Verdière, R. Panneton, S. Elkoun, T. Dupont, and P. Leclaire, "Comparison between parallel transfer matrix method and admittance sum method," *The Journal of the Acoustical Society of America*, vol. 136, no. 2, EL90–EL95, 2014.

[27] J. Kennedy and R. Eberhart, "Particle swarm optimization," in *Proceedings of the IEEE International Conference on Neural Networks (ICNN'95)*, IEEE, vol. 4, 1995, pp. 1942–1948.

[28] Y. Shi and R. Eberhart, "A modified particle swarm optimizer," in *Proceedings of the 1998 IEEE International Conference on Evolutionary Computation*, IEEE, 1998, pp. 69–73.

[29] R. C. Eberhart and Y. Shi, "Comparing inertia weights and constriction factors in particle swarm optimization," in *Proceedings of the 2000 IEEE Congress on Evolutionary Computation (CEC 2000)*, IEEE, vol. 1, 2000, pp. 84–88.

[30] M. Clerc and J. Kennedy, "The particle swarm-explosion, stability, and convergence in a multidimensional complex space," *IEEE Transactions on Evolutionary Computation*, vol. 6, no. 1, pp. 58–73, 2002.

[31] I. O. for Standardization, *Iso 10534-2. acoustics—determination of sound absorption coefficient and impedance in impedance tubes*, 2001.

[32] G. Catapane, G. Petrone, and O. Robin, "Series and parallel coupling of 3d printed micro-perforated panels and coiled quarter wavelength tubes," *The Journal of the Acoustical Society of America*, vol. 154, no. 5, pp. 3027–3040, 2023.